

# Hydrogen Bonding in 2,3-Dithiolatoterephthaldiamide Complexes of Cobalt(III), Nickel(II), and Iron(III)

F. Ekkehardt Hahn,\*<sup>[a]</sup> Thomas Eiting,<sup>[a]</sup> Wolfram W. Seidel,<sup>[a]</sup> and Tania Pape<sup>[a]</sup>

*Dedicated to Professor Uwe Rosenthal on the occasion of his 60th birthday*

**Keywords:** Dithiolenes / Hydrogen bonding / X-ray diffraction / Cobalt / Nickel / Iron

The synthesis and characterization of the novel 2,3-dithiolatoterephthaldiamide ligands  $C_6H_2[C(O)NHBn]_2(SH)_2$  (**H<sub>2</sub>-1a**) and  $C_6H_2[C(O)NH-iPr]_2(SH)_2$  (**H<sub>2</sub>-1b**) as well as their complexes with  $Ni^{II}$ ,  $Co^{III}$ , and  $Fe^{III}$  is described. The molecular structures of the complexes  $(NEt_4)[Co(\mathbf{1a})_2]$ ,  $(AsPh_4)_2[Ni(\mathbf{1b})_2] \cdot dmf$ , and  $(AsPh_4)[Fe(\mathbf{1a})_2] \cdot CH_2Cl_2$  were determined by single-crystal X-ray diffraction. Electronic absorption spectroscopy and cyclic voltammetry were applied to investigate

the electronic properties of the complex anions  $[M(L)_2]^{n-}$  ( $M = Ni, Co; L = \mathbf{1a}, \mathbf{1b}; n = 1, 2$ ). Comparison of the structural and electronic characteristics of the complexes with ligands **1a**<sup>2-</sup> and **1b**<sup>2-</sup> to those of the corresponding complexes with related benzene-*o*-dithiolato ligands indicates a notable influence of intramolecular N–H...S hydrogen bonding between amide protons and coordinated sulfur atoms in 2,3-dithiolatoterephthalamide complexes.

## Introduction

During the last decades (dithiolene)metal complexes have attracted considerable interest owing to their distinctive molecular and electronic structures.<sup>[1]</sup> In addition, their biological relevance<sup>[2]</sup> and potential applications in materials science<sup>[3]</sup> with respect to photonics, electronic conductors and magnetochemistry have stimulated further investigations. Recent comprehensive studies of the electronic structure of square-planar bis(benzene-*o*-dithiolato) complexes confirmed the non-innocent nature of enedithiolato ligands showing that they can form *S,S*-coordinated dithio(1-)  $\pi$ -radical anions by intramolecular redox processes.<sup>[4]</sup>

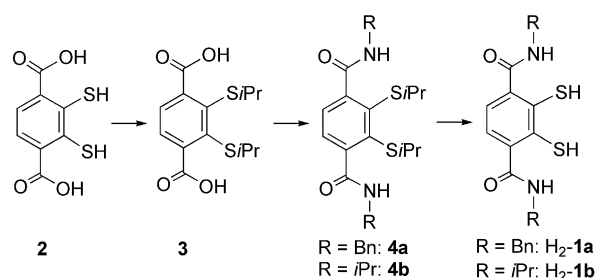
Our research in the field of enedithiolates is driven by attempts to incorporate the benzene-*o*-dithiolato binding unit into larger polydentate ligands and to use these for the generation of metallocsupramolecular assemblies like triple-stranded homo- and heterodimetallic helicates<sup>[5a–5j]</sup> or polynuclear clusters.<sup>[5k–5m]</sup> In these efforts, 2,3-dimercaptoterephthalic acid is a particularly valuable building block due to the functionalization of the benzene-*o*-dithiol in both *ortho* positions. In addition, intermolecular hydrogen bonding has been shown to be of importance for the formation of solid-state networks from nickel complexes with suitably functionalized dithiolene ligands.<sup>[6]</sup>

In this contribution we present the first nickel(II), cobalt(III), and iron(III) complexes with 2,3-dithiolatoterephthaldiamide ligands. The molecular structures as well as the electronic properties of these complexes are compared with the prototype complexes of the unsubstituted benzene-*o*-dithiolato ligand (**bdt**<sup>2-</sup>). The goal of this work was to investigate the influence of the amide substituents on the molecular structures and the electronic properties of the resulting (benzene-*o*-dithiolato)metal complexes.

## Results and Discussion

### Synthesis of Ligands and Complexes

The ligands **H<sub>2</sub>-1a** and **H<sub>2</sub>-1b** were prepared by using a protocol described previously (Scheme 1).<sup>[7]</sup> 2,3-Dimercaptoterephthalic acid (**2**)<sup>[7a]</sup> was converted into the *S,S*-dialkylated derivative **3** in order to protect the thiol groups. Subsequently, the terephthaldiamides **4a** and **4b** were pre-

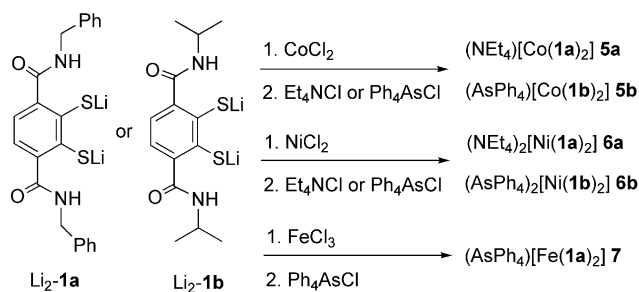


Scheme 1. Synthesis of ligands **H<sub>2</sub>-1** and **H<sub>2</sub>-2**.

[a] Institut für Anorganische und Analytische Chemie, Westfälische Wilhelms-Universität Münster, Corrensstraße 30, 48149 Münster, Germany  
Fax: +49-251-833-3108  
E-mail: fehahn@uni-muenster.de

pared by conventional amide synthesis using either benzyl- or isopropylamine. Cleavage of the *S*-isopropyl bonds in **4a** and **4b** with sodium/naphthalene in thf yielded, after hydrolysis, the ligands **H<sub>2</sub>-1a** and **H<sub>2</sub>-1b**, respectively.<sup>[5,7]</sup>

Reaction of the metal salts  $\text{CoCl}_2 \cdot 6\text{H}_2\text{O}$  or  $\text{NiCl}_2 \cdot 6\text{H}_2\text{O}$  with 2 equiv. of either **H<sub>2</sub>-1a** or **H<sub>2</sub>-1b**, respectively, in methanol in the presence of 4 equiv. of LiOMe gave red-brown solutions in all cases. For  $\text{M} = \text{Co}$  the solutions immediately turned deep blue upon aerial oxidation, indicating the formation of the  $\text{Co}^{\text{III}}$  complexes  $\text{Li}[\text{Co}(\mathbf{1a})_2]$  and  $\text{Li}[\text{Co}(\mathbf{1b})_2]$ . The corresponding nickel compounds on the other hand were isolated under anaerobic conditions as  $\text{Ni}^{\text{II}}$  complexes  $\text{Li}_2[\text{Ni}(\mathbf{1a})_2]$  or  $\text{Li}_2[\text{Ni}(\mathbf{1b})_2]$ . After cation exchange with either  $\text{Et}_4\text{NCl}$  or  $\text{Ph}_4\text{AsCl}$  in methanol solution, complexes  $(\text{Et}_4\text{N})[\text{Co}^{\text{III}}(\mathbf{1a})_2]$  (**5a**),  $(\text{Ph}_4\text{As})[\text{Co}^{\text{III}}(\mathbf{1b})_2]$  (**5b**),  $(\text{Et}_4\text{N})_2[\text{Ni}^{\text{II}}(\mathbf{1a})_2]$  (**6a**), and  $(\text{Ph}_4\text{As})_2[\text{Ni}^{\text{II}}(\mathbf{1b})_2]$  (**6b**) were isolated as blue solids in the case of the cobalt complexes and as red solids in the case of the nickel complexes (Scheme 2). Salts **5a** and **6a** with the *N*-benzylamide substituents are only soluble in highly polar solvents such as dmf (dmf = *N,N'*-dimethylformamide), whereas **5b** and **6b** with *N*-isopropylamide substituents are soluble in less polar solvents like  $\text{CH}_2\text{Cl}_2$  and  $\text{CHCl}_3$ . Interestingly, the substitution pattern at the amide functionality and the type of the counterion has a stronger influence on the solubility than the charge of the complex anions. The  $\text{Fe}^{\text{III}}$  complex  $(\text{Ph}_4\text{As})[\text{Fe}(\mathbf{1a})_2]$  (**7**), was prepared in an analogous procedure by using  $\text{FeCl}_3$  as metal precursor (Scheme 2).



Scheme 2. Preparation of the metal complexes.

## Molecular Structures

The molecular structures of **5a**, **6b** and **7** have been determined by X-ray diffraction analysis. Single crystals of **5a** and **6b**·dmf were obtained by vapor diffusion of diethyl ether into saturated solutions of the complexes in dmf. Vapor diffusion of diethyl ether into a concentrated dichloromethane solution of **7** yielded crystals of  $\mathbf{7} \cdot 2\text{CH}_2\text{Cl}_2$ , which were suitable for an X-ray diffraction study.

The molecular structure of the complex anion  $[\text{Co}(\mathbf{1a})_2]^-$  in **5a** is depicted in Figure 1, and selected bond lengths are listed in Table 1. The complex anion shows an overall square-planar coordination geometry. The Co–S and C–S distances fall in the typical range and match those reported for  $[\text{Co}(\text{S}_2\text{C}_6\text{H}_4)_2]^-$ <sup>[8a]</sup> and  $[\text{Co}(\text{S}_2\text{C}_6\text{H}_3\text{CH}_3)_2]^-$ <sup>[8b]</sup>

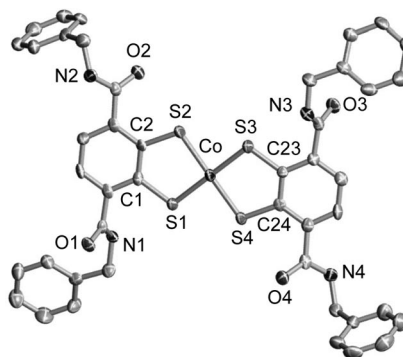


Figure 1. Molecular structure of the anion  $[\text{Co}(\mathbf{1a})_2]^-$  in **5a**. Thermal ellipsoids are drawn at the 50% probability level (hydrogen atoms and cations have been omitted for clarity). Selected bond angles [°]: S1–Co–S2 91.43(5), S1–Co–S3 179.72(7), S1–Co–S4, 88.45(5), S2–Co–S3 88.65(5), S2–Co–S4 178.15(6), S3–Co–S4 91.46(5), Co–S1–C1 105.05(15), Co–S2–C2 105.20(14), Co–S3–C23 104.72(14), Co–S4–C24 105.16(14).

Table 1. Selected bond lengths [Å] in **5a**, **6b**·dmf and  $\mathbf{7} \cdot 2\text{CH}_2\text{Cl}_2$ .

	<b>5a</b> (M = Co)	<b>6b</b> (M = Ni) <sup>[a]</sup>	<b>6b</b> (M = Ni) <sup>[a]</sup>	<b>7</b> (M = Fe)
M–S1 <sup>[b]</sup>	2.162(1)	2.144(1)	2.147(1)	2.220(1)
M–S2 <sup>[b]</sup>	2.172(1)	2.148(1)	2.139(1)	2.231(1)
M–S3	2.163(1)			2.212(1)
M–S4	2.169(1)			2.244(1)
M–S4*				2.494(1)
C1–S1 <sup>[b]</sup>	1.758(4)	1.764(4)	1.759(3)	1.748(4)
C2–S2 <sup>[b]</sup>	1.771(4)	1.754(3)	1.761(4)	1.766(4)
C23–S3	1.750(4)			1.757(4)
C24–S4	1.765(4)			1.768(4)
C1–C2 <sup>[b]</sup>	1.401(6)	1.415(5)	1.421(5)	1.408(6)
C23–C24	1.399(5)			1.402(6)

[a] The asymmetric unit contains two crystallographically independent halves of the formula unit of **6b**, both nickel atoms reside on crystallographic inversion centers. [b] For M = Ni: C21, C22, S21 and S22.

Alternatively, cobalt(III) complexes bearing electron-withdrawing benzene-*o*-dithiolato ligands like  $\text{S}_2\text{C}_6\text{Cl}_4^{2-}$  or  $\text{S}_2\text{C}_6\text{H}_2(\text{CN})_2^{2-}$  have been reported to dimerize.<sup>[9]</sup> Such dimers are formed by  $\mu_2$ -coordination of a single sulfur atom of an individual  $\text{CoS}_4$  moiety to the apical position of a second  $\text{CoS}_4$  unit and vice versa. Surprisingly, in spite of the electron-withdrawing nature of the amide substituents, no such intermolecular interactions have been observed for **5a**. In the solid state the anions of **5a** are connected by intermolecular N–H⋯O hydrogen bonds between amide groups (shortest N⋯O distance 2.75 Å). The  $\text{CoS}_4$  moieties are well separated, and the closest intermolecular Co⋯S distances measure more than 8 Å.

The molecular structure of the dianion  $[\text{Ni}(\mathbf{1b})_2]^{2-}$  in **6b**·dmf is shown in Figure 2, and selected bond lengths are listed in Table 1. The asymmetric unit of **6b**·dmf contains two independent halves of the complex dianion, two  $\text{Ph}_4\text{As}^+$  cations and one dmf molecule. Only one of the essentially identical complex anions in the unit cell is depicted in Figure 2. As expected, the nickel centers in the two independent molecules of **6b** are surrounded by two benzene-*o*-dithiolato ligands in a square-planar fashion. The Ni–S

bond lengths, which fall in the range between 2.139(1) and 2.148(1) Å, are somewhat shorter than those reported for the comparable Ni<sup>II</sup> complex dianions [Ni(bdt)<sub>2</sub>]<sup>2-</sup> [2.168(4)–2.181(4)]<sup>[10]</sup> and [Ni{S<sub>2</sub>C<sub>6</sub>H<sub>2</sub>(*t*Bu)<sub>2</sub>}<sub>2</sub>]<sup>2-</sup> [2.172(1) and 2.175(1)].<sup>[11]</sup> In addition, the chelate rings in [Ni(**1b**)<sub>2</sub>]<sup>2-</sup> are folded about the S–S vector (Figure 2, bottom). For example, the angle between the planes S1–Ni1–S2 and S1–C1–C2–S2 measures 16.7°. Such a folding is rather atypical for bis(benzene-*o*-dithiolato) group 10 metal complexes but has been observed regularly for titanium complexes bearing bdt<sup>2-</sup> ligands.<sup>[5]</sup> In contrast to the situation found for **5a**, the NH groups of the amide substituents in **6b** are directed towards the sulfur atoms. The intramolecular N···S distances measure about 2.96 Å indicating an intramolecular N–H···S hydrogen-bond interaction. This observation can be attributed to the higher charge of the [Ni(**1b**)<sub>2</sub>]<sup>2-</sup> dianion compared to the monoanion [Co(**1a**)<sub>2</sub>]<sup>-</sup> where no indications for intramolecular N–H···S interactions have been found in the solid state.

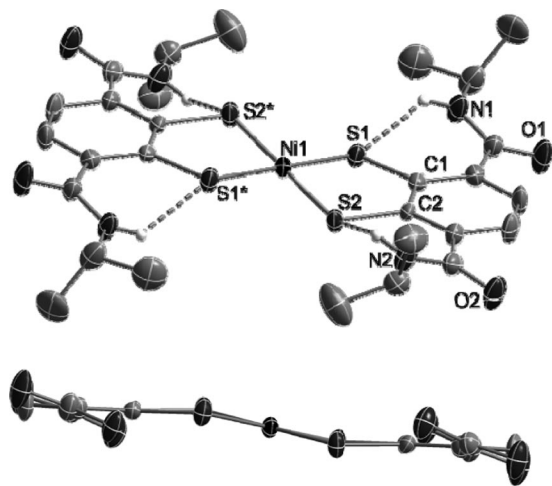


Figure 2. Molecular structure of the dianion [Ni(**1b**)<sub>2</sub>]<sup>2-</sup> in **6b**·dmf. Thermal ellipsoids are drawn at the 50% probability level (carbon-bound hydrogen atoms, cations and solvent molecules have been omitted for clarity). Selected bond angles [°] for molecule 1 [molecule 2]: S1–Ni1–S2 89.57(4) [90.40(4)], S1–Ni1–S2\* 90.43(4) [89.60(3)], N1–S1–C1 107.14(12) [106.76(12)], N1–S2–C2 107.04(13) [106.39(12)].

The X-ray analysis showed that the anions of compound **7**·CH<sub>2</sub>Cl<sub>2</sub> dimerize in the solid state with formation of the dinuclear dianion [Fe(**1a**)<sub>2</sub>]<sup>2-</sup>. This dianion resides on a crystallographic inversion center (Figure 3, Table 1). The dimerization has been expected since bis(benzene-*o*-dithiolato)iron complexes are only monomeric with iron(II),<sup>[12]</sup> whereas the corresponding iron(III) complexes dimerize<sup>[13]</sup> regardless of the electron-withdrawing or -donating character of the substituents at the benzene-*o*-dithiolato donor groups.<sup>[14]</sup> The complex anion [Fe(**1a**)<sub>2</sub>]<sup>2-</sup> consists of two FeS<sub>4</sub> moieties, which are linked by two intermolecular Fe–S–Fe bridges leading to a distorted square-pyramidal coordination at each iron atom. In addition, the two [Fe(**1a**)<sub>2</sub>]<sup>-</sup> subunits are connected by hydrogen bonds between the amide groups (Figure 3; O2···N3\* 2.854 Å, N1···O4\*

2.901 Å). Contrary to this observation, the cobalt(III) complex anion [Co<sup>III</sup>(**1a**)]<sup>-</sup> in **5a**, possessing the same charge as [Fe(**1a**)<sub>2</sub>]<sup>-</sup>, shows no tendency for a dimerization by either intermolecular Co–S interactions or by N–H···O hydrogen bonding.

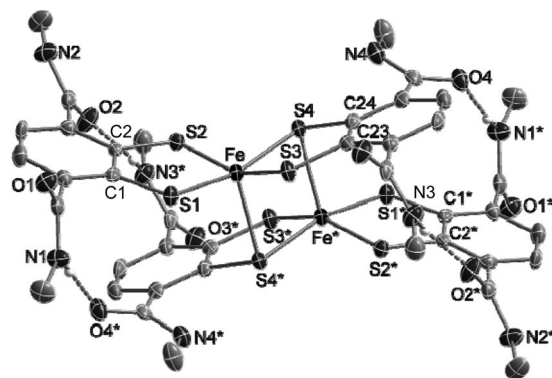


Figure 3. Molecular structure of the dianion [Fe(**1a**)<sub>2</sub>]<sup>2-</sup> in 7·2CH<sub>2</sub>Cl<sub>2</sub> formed from two formula units of **7**. Thermal ellipsoids are drawn at the 50% probability level (carbon-bound hydrogen atoms, cations, solvent molecules and the phenyl groups of the benzyl amide substituents have been omitted for clarity). Selected bond angles [°]: S1–Fe–S2 88.71(5), S1–Fe–S3 87.60(5), S1–Fe–S4 164.31(5), S2–Fe–S3 155.53(5), S2–Fe–S4 89.01(5), S3–Fe–S4 88.07(5), S1–Fe–S4\* 99.89(5), S2–Fe–S4\* 103.95(5), S3–Fe–S4\* 100.52(5), S4–Fe–S4\* 95.72(5), Fe–S4–Fe\* 84.28(5), Fe–S1–C1 106.9(2), Fe–S2–C2 106.3(2), Fe–S3–C23 107.1(2), Fe–S4–C24 107.01(2).

The bond lengths and angles within the Fe<sub>2</sub>S<sub>8</sub> core of the [Fe(**1a**)<sub>2</sub>]<sup>2-</sup> anion match those found in similar complexes described in the literature.<sup>[13,14]</sup> The distinctively long Fe–S4\* bond in the apical position (Table 1) indicates the weakness of the interaction, which is corroborated by the recent isolation of the mononuclear, base-stabilized Fe<sup>III</sup> complex [Fe(bdt)<sub>2</sub>(thf)]<sup>-</sup>.<sup>[15]</sup> The chelate rings in [Fe(**1a**)<sub>2</sub>]<sup>-</sup> are essentially planar.

## Electronic Properties

Quasi-reversible electron-transfer waves (peak-to-peak potential differences 82–107 mV) for the redox couples [ML<sub>2</sub>]<sup>2-</sup>/[ML<sub>2</sub>]<sup>-</sup> with M = Co<sup>III</sup> and Ni<sup>II</sup> and L = **1a**<sup>2-</sup> and **1b**<sup>2-</sup> (Figure 4) allowed an estimation of the half-wave potentials. The *E*<sub>1/2</sub> values are listed in Table 2 together with those of related benzene-*o*-dithiolato complexes. The half-wave potentials of the cobalt complexes in dmf were determined as *E*<sub>1/2</sub> = –1040 mV for **5a** and *E*<sub>1/2</sub> = –1080 mV for **5b** (vs. Fc<sup>+</sup>/Fc in all cases). These half-wave potentials fall in between the *E*<sub>1/2</sub> values reported for the redox couples of [Co{S<sub>2</sub>C<sub>6</sub>H<sub>3</sub>C(O)NHR}<sub>2</sub>]<sup>2-/–</sup> bearing benzene-*o*-dithiolato ligands with only one amide substituent<sup>[16]</sup> and [Co(S<sub>2</sub>C<sub>6</sub>Cl<sub>4</sub>)<sub>2</sub>]<sup>2-/–</sup> bearing two tetrachloro-substituted benzene-*o*-dithiolato ligands.<sup>[17]</sup> This observation can be rationalized by the relative strength of the inductive effects of the substituents at the benzene-*o*-dithiolato ligand. The formal addition of an amide substituent to the benzene-*o*-dithiolato ligands causes a change of the potential of approxi-

mately 0.12 V for the bis(benzene-*o*-dithiolato)cobaltate complexes. The whole potential range, marked by the electron-poor  $[\text{Co}\{\text{S}_2\text{C}_6\text{H}_2(\text{CN})_2\}_2]^{2-/-}$  with two electron-withdrawing cyano groups<sup>[9a]</sup> and the electron-rich  $[\text{Co}(\text{S}_2\text{C}_6\text{Me}_4)]^{2-/-}$  with four electron-donating methyl groups,<sup>[17]</sup> spans more than 1.0 V, indicating the strong influence of the ligand substitution on the redox potential in this type of complexes. The order of potentials in Table 2 reveals that to date complex anion  $[\text{Co}(\mathbf{1a})_2]^-$  represents the upper potential limit for mononuclear  $[\text{Co}(\text{S}_2\text{C}_6\text{X}_4)_2]^-$  complexes, since complexes with even more electron-poor benzene-*o*-dithiolato ligands such as  $[\text{Co}(\text{S}_2\text{C}_6\text{Cl}_4)_2]^-$  or  $[\text{Co}\{\text{S}_2\text{C}_6\text{H}_2(\text{CN})_2\}_2]^-$  have been found to dimerize in the solid state.<sup>[9]</sup>

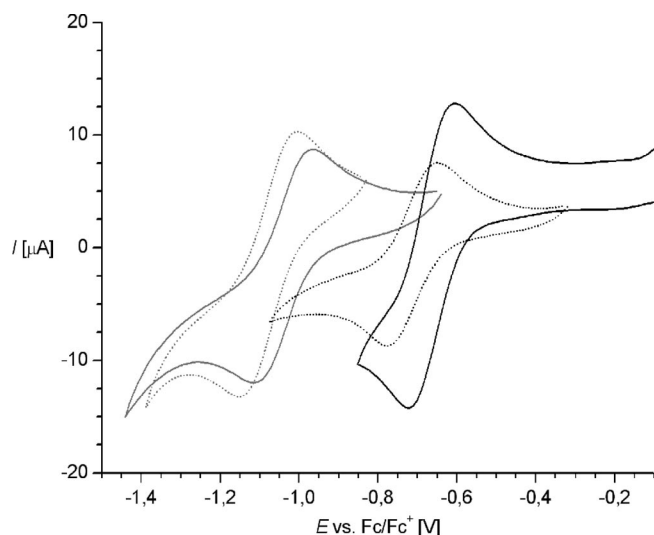


Figure 4. Cyclic voltammograms of **5a** (gray line), **5b** (gray dotted line), **6a** (black line), **6b** (black dotted line), solvent dmf, scan rate 100 mV·s<sup>-1</sup>.

Table 2. Electronic data of bis(benzene-*o*-dithiolato)metal complexes.

L in $[\text{ML}_2]^-$	$E_{1/2}$ [V] vs. $\text{Fc}/\text{Fc}^+$		$\lambda$ ( $1b_{1u} \rightarrow 2b_{2g}$ ) [nm]	
	M = Co	M = Ni	M = Co	M = Ni
$\text{S}_2\text{C}_6\text{Me}_4^{2-}$ <sup>[7]</sup>	-1.48 <sup>[a]</sup>	-1.15 <sup>[a]</sup>	680 <sup>[b]</sup>	926 <sup>[b]</sup>
$\text{S}_2\text{C}_6\text{H}_2(\text{tBu})_2^{2-}$ <sup>[4a,17]</sup>	-1.10	-1.10	671 <sup>[b]</sup>	890 <sup>[b]</sup>
$\text{S}_2\text{C}_6\text{H}_3\text{Me}^{2-}$ <sup>[13a,17]</sup>	-1.31 <sup>[a]</sup>	-0.97 <sup>[a]</sup>	660 <sup>[b]</sup>	860 <sup>[c]</sup>
$\text{S}_2\text{C}_6\text{H}_4^{2-}$ <sup>[17]</sup>	-1.28 <sup>[a]</sup>	-0.95 <sup>[a]</sup>	657 <sup>[b]</sup>	881 <sup>[b]</sup>
$\text{S}_2\text{C}_6\text{H}_3\text{C}(\text{O})\text{NHR}^{2-}$ <sup>[16]</sup>	-1.16 <sup>[d]</sup>	-0.78 <sup>[d]</sup>	653 <sup>[b]</sup>	860 <sup>[d]</sup>
<b>1a</b> <sup>2-</sup>	-1.04 <sup>[d]</sup>	-0.66 <sup>[d]</sup>	654 <sup>[e]</sup>	870 <sup>[e]</sup>
<b>1b</b> <sup>2-</sup>	-1.08 <sup>[d]</sup>	-0.71 <sup>[d]</sup>	662 <sup>[e]</sup>	864 <sup>[e]</sup>
$\text{S}_2\text{C}_6\text{Cl}_4^{2-}$ <sup>[17]</sup>	-0.75 <sup>[f]</sup>	-0.43 <sup>[a]</sup>	667 <sup>[b]</sup>	885 <sup>[b]</sup>
$\text{S}_2\text{C}_6\text{H}_2(\text{CN})_2^{2-}$ <sup>[9a]</sup>	-0.31 <sup>[f]</sup>	-0.02 <sup>[f]</sup>		

[a] Adjusted according to ref.<sup>[18]</sup> to  $\text{Fc}/\text{Fc}^+$  standard; originally measured vs.  $\text{Ag}/\text{AgClO}_4$  in dmf. [b] Dichloromethane solution. [c] MeCN solution. [d] dmf solution. [e] MeOH solution. [f] Adjusted according to ref.<sup>[18]</sup> to  $\text{Fc}/\text{Fc}^+$  standard; originally measured vs.  $\text{Ag}/\text{AgNO}_3$  in MeCN.

Given the relative moderate potential changes caused by addition of amide groups to the benzene-*o*-dithiolato ligands (120 mV for cobaltate complexes for the transition from monoamide-substituted benzene-*o*-dithiolato ligands to

diamide-substituted benzene-*o*-dithiolato ligands) we became interested in the influence of the particular type of amide, *N*-benzylamide in **1a**<sup>2-</sup> and *N*-isopropylamide in **1b**<sup>2-</sup>. For the cobaltate complexes **5a** and **5b** the half-wave potentials differed by 40 mV (Figure 4, Table 2). The same effect is observed with the nickel complexes where estimated values of  $E_{1/2} = -660$  mV for **6a** and  $E_{1/2} = -710$  mV for **6b** were recorded (Figure 4, Table 2).

Intramolecular N–H···S hydrogen bonds, which have been observed in the solid-state structure of  $[\text{Ni}(\mathbf{1b})_2]^{2-}$  in **6b**·dmf most likely account for this difference. The higher acidity of *N*-benzylamides relative to *N*-isopropylamides leads to a better hydrogen-donor ability of the former. The underlying difference is evident, for instance, in the <sup>1</sup>H NMR spectra of the diamides **4a** and **4b** in  $\text{CDCl}_3$ , in which the signal of the amide protons appears at  $\delta = 7.04$  ppm for the *N*-benzylamide and at  $\delta = 6.35$  ppm for the *N*-isopropylamide. The latter resonance is low-field-shifted to  $\delta = 7.75$  ppm for  $(\text{Ph}_4\text{As})_2[\text{Ni}(\mathbf{1b})_2]$  measured likewise in  $\text{CDCl}_3$ . Unfortunately,  $(\text{Et}_4\text{N})_2[\text{Ni}(\mathbf{1a})_2]$  is not soluble in  $\text{CDCl}_3$  to allow a comparison. A stronger intramolecular N–H···S interaction would stabilize the lower oxidation state due to a charge reduction at the sulfur atoms. Therefore, the bis(benzene-*o*-dithiolato) complexes with four *N*-benzylamide substituents (**5a** and **6a**) are easier to reduce as indicated by the higher  $E_{1/2}$  values. The adjustment of the redox potential by hydrogen bonding to sulfur atoms has been found to be an essential property for the function of iron–sulfur proteins.<sup>[19]</sup>

For the measurement of the electronic spectra, the nickel complexes **6a** and **6b** were oxidized by air in order to observe the typical low-energy charge-transfer bands. The UV/Vis spectroscopic data of  $(\text{Et}_4\text{N})[\text{Ni}^{\text{III}}(\mathbf{1a})_2]$ ,  $(\text{Ph}_4\text{As})[\text{Ni}^{\text{III}}(\mathbf{1b})_2]$  and those of the corresponding cobalt(III) complexes **5a** and **5b** are compared with data of related complexes from the literature in Table 2. From Table 2 it is evident that the position of the dominant charge-transfer bands in the visible region varies only slightly with the ligand type. In addition, no clear trend can be derived, which is in contrast to the trends observed for the redox potentials. Recent comprehensive calculations by Neese and Wieghardt et al. on bis(benzene-*o*-dithiolato) complexes led to the conclusion that these  $1b_{1u} \rightarrow 2b_{2g}$  transitions are ligand-to-ligand (LLCT) in character with nickel<sup>[4a]</sup> and of mixed nature ligand-to-ligand (LLCT) and ligand-to-metal (LMCT) with cobalt.<sup>[12a]</sup> These results corroborate our observation that a particular type of ligand influences the redox potential, whereas the same does not apply to the charge-transfer bands.

## Conclusions

In search for new transition metal complexes with benzene-*o*-dithiolato ligands we have synthesized the diamide-functionalized derivatives **H<sub>2</sub>-1a** and **H<sub>2</sub>-1b** derived from terephthalic acid. These ligands form bis(benzene-*o*-dithiolato) complexes with  $\text{Fe}^{\text{III}}$ ,  $\text{Co}^{\text{III}}$ , and  $\text{Ni}^{\text{II}}$ , which adopt the



expected square-planar coordination geometry with Ni<sup>II</sup> and Co<sup>III</sup> and a square-pyramidal geometry with Fe<sup>III</sup> due to dimerization of the anion [Fe(**1a**)<sub>2</sub>]<sup>−</sup> to the dinuclear dianion [Fe(**1a**)<sub>2</sub>]<sub>2</sub><sup>2−</sup>. No such dimerization has been observed for the Co<sup>III</sup> congener. This observation indicates that the dimerization for M = Co<sup>III</sup> is restricted to complexes bearing benzene-*o*-dithiolato ligands with strongly electron-withdrawing substituents. In this context, cyclic voltammetry studies allowed the classification of the new 1,2-dithiolatoterephthaldiamide ligands on the redox scale of related benzene-*o*-dithiolato ligands. In addition, our studies revealed an influence of the particular amide type on the redox potential of the coordinated metal center. This effect can be attributed to intramolecular N–H⋯S hydrogen interactions, which are evident in the solid-state structure of (Ph<sub>4</sub>As)<sub>2</sub>[Ni(**1b**)<sub>2</sub>].

## Experimental Section

**Materials and Methods:** If not stated otherwise, all manipulations were performed under dry argon by means of standard Schlenk techniques. Solvents were dried by standard methods and freshly distilled prior to use. *N,N,N',N'*-Tetramethylethylenediamine (TMEDA) was purified by vacuum distillation from Na/benzophenone. <sup>1</sup>H and <sup>13</sup>C NMR spectra were recorded with a Bruker AC200 NMR spectrometer. Mass spectra were obtained with a Bruker Reflex IV spectrometer. UV/Vis spectra were measured with a Varian Cary 50 spectrometer. Cyclic voltammetry data were acquired with an ECO/Metrohm PGSTAT30 potentiometer with a platinum working electrode, an Ag/AgCl double-junction electrode (3 M KCl solution) as the reference electrode and Bu<sub>4</sub>NBF<sub>4</sub> as the supporting electrolyte. Benzene-*o*-dithiol was prepared according to a literature procedure.<sup>[20]</sup> Consistent microanalytical data for complex **5–7** were difficult to obtain. However, all complexes have been fully characterized by either NMR spectroscopy or mass spectrometry in addition to X-ray diffraction studies on **5a**, **6b**·dmf and **7**·CH<sub>2</sub>Cl<sub>2</sub>.

**2,3-Bis(isopropylmercapto)terephthalic Acid (3):** Benzene-*o*-dithiol (4 mL, 34.8 mmol) was added to a solution of TMEDA (26 mL, 174 mmol) and *n*BuLi (10 M solution in *n*-hexane) (17.4 mL, 174 mmol) in *n*-hexane (100 mL) at 0 °C. After stirring at room temperature for 90 h, dry CO<sub>2</sub> was passed through the mixture at 0 °C for 2 h. After evaporation of the solvent, the residue was dissolved in methanol (100 mL), and isopropyl bromide (9.8 mL, 104.4 mmol) was added. The mixture was heated under reflux for 24 h. After evaporation of the methanol, the residue was dissolved in water and acidified with hydrochloric acid (37%) to pH = 2. The aqueous solution was extracted with diethyl ether (3 × 50 mL), and the combined organic layers were dried with MgSO<sub>4</sub>. Volatiles were removed in vacuo to afford a brown oil. Isolation of **3** was achieved by column chromatography on SiO<sub>2</sub> using diethyl ether/petroleum ether/acetic acid (3:1:0.2) as the eluent. Compound **3** was obtained as a pale yellow powder (2.3 g, 7.3 mmol, 21%). <sup>1</sup>H NMR (200 MHz, CDCl<sub>3</sub>, 25 °C): δ = 9.78 (s, 2 H, CO<sub>2</sub>H), 7.95 (s, 2 H, Ar-H), 3.59 (sept, 2 H, SCH), 1.26 (d, 12 H, CH<sub>3</sub>) ppm. <sup>13</sup>C NMR (50.32 MHz, CDCl<sub>3</sub>, 25 °C): δ = 169.2 (CO<sub>2</sub>H), 140.6, 139.8, 130.3 (Ar-C), 42.8 (SCH), 31.0 (CH<sub>3</sub>) ppm.

***N,N'*-Dibenzyl-2,3-bis(isopropylmercapto)terephthalamide (4a) and *N,N'*-Diisopropyl-2,3-bis(isopropylmercapto)terephthalamide (4b):** A mixture of compound **3** (1.47 g, 4.68 mmol), CHCl<sub>3</sub> (20 mL),

SOCl<sub>2</sub> (1.5 mL) and a few drops of dmf was heated under reflux for 2 h. The oily terephthalic dichloride obtained after removal of the solvent was dissolved in thf (20 mL), and the resulting solution was added to a solution of either benzylamine (1.02 mL, 9.34 mmol) or isopropylamine (0.83 mL, 9.34 mmol) and NEt<sub>3</sub> (2 mL, 14.35 mmol) in thf (20 mL). After stirring at room temperature for 12 h, the reaction mixture was filtered, and the filtrate was concentrated to dryness in vacuo. The residue was washed with water and diethyl ether (**4a**) or *n*-hexane (**4b**) to obtain a white solid. **4a**: Yield: 1.75 g (75%). <sup>1</sup>H NMR (200 MHz, CDCl<sub>3</sub>, 25 °C): δ = 7.43–7.18 (m, 12 H, Ar-H), 7.04 [t, 2 H, C(O)NH], 4.62 (d, 4 H, NCH<sub>2</sub>Ph), 3.42 (sept, 2 H, SCH), 1.13 (d, 12 H, CH<sub>3</sub>) ppm. <sup>13</sup>C NMR (50.32 MHz, CDCl<sub>3</sub>, 25 °C): δ = 167.7 [C(O)NH], 143.6, 138.0, 137.6, 129.0, 128.7, 128.2, 127.6 (Ar-C), 44.2 (NCH<sub>2</sub>Ph), 41.4 (SCH), 22.8 (CH<sub>3</sub>) ppm. **4b**: Yield: 1.56 g (84%). <sup>1</sup>H NMR (200 MHz, CDCl<sub>3</sub>, 25 °C): δ = 7.49 (s, 2 H, Ar-H), 6.35 [d, 2 H, C(O)NH], 4.20 (sept, 2 H, NCH), 3.44 (sept, 2 H, SCH), 1.20 (d, 12 H, CH<sub>3</sub>), 1.15 (d, 12 H, CH<sub>3</sub>) ppm. <sup>13</sup>C NMR (50.32 MHz, CDCl<sub>3</sub>, 25 °C): δ = 166.8 [C(O)NH], 143.6, 137.5, 128.6 (Ar-C), 41.8 (NCH), 41.0 (SCH), 22.7 (CH<sub>3</sub>), 22.3 (CH<sub>3</sub>) ppm.

***N,N'*-Dibenzyl-2,3-dimercaptoterephthalamide (H<sub>2</sub>-1a) and *N,N'*-Diisopropyl-2,3-dimercaptoterephthalamide (H<sub>2</sub>-1b):** Compound **4a** (1.5 g, 3.06 mmol) and naphthalene (1.18 g, 9.18 mmol) were dissolved in thf (80 mL), and pieces of sodium (420 mg, 18.36 mmol) were added. The mixture was stirred at ambient temperature for 12 h, and then methanol (10 mL) was added dropwise. After 10 min, the solvents were removed in vacuo, the residue was dissolved in degassed water (20 mL), and the mixture was filtered. The aqueous filtrate was washed with diethyl ether (3 × 10 mL) and acidified with hydrochloric acid (37%) to afford a white solid. The precipitate was filtered off and washed with water (2 × 20 mL) and diethyl ether (2 × 10 mL). Drying in vacuo yielded H<sub>2</sub>-**1** as a white powder (0.85 g, 68%). <sup>1</sup>H NMR (200 MHz, CDCl<sub>3</sub>, 25 °C): δ = 9.15 [t, 2 H, C(O)NH], 7.77–7.44 (m, 12 H, Ar-H), 4.62 (d, 4 H, NCH<sub>2</sub>Ph), 3.98 (s br, 2 H, SH) ppm. <sup>13</sup>C NMR (50.32 MHz, CDCl<sub>3</sub>, 25 °C): δ = 169.5 [C(O)NH], 139.9, 136.4, 133.8, 127.6, 127.2, 124.9 (Ar-C), 43.7 (NCH<sub>2</sub>Ph) ppm. The same procedure for **4b** (0.8 g, 2.0 mmol) gave H<sub>2</sub>-**1b** (0.54 g, 86%). <sup>1</sup>H NMR (200 MHz, CDCl<sub>3</sub>, 25 °C): δ = 8.52 [d, 2 H, C(O)NH], 7.87 (s, 2 H, Ar-H), 4.92 (br. s, 2 H, SH), 4.03 (sept, 2 H, NCH), 1.16 (d, 12 H, CH<sub>3</sub>) ppm. <sup>13</sup>C NMR (50.32 MHz, CDCl<sub>3</sub>, 25 °C): δ = 167.3 [C(O)NH], 136.0, 132.1, 124.0 (Ar-C), 41.0 (NCH), 22.0 (CH<sub>3</sub>) ppm.

**(Et<sub>4</sub>N)[Co(**1a**)<sub>2</sub>] (5a):** A solution of H<sub>2</sub>-**1a** (340 mg, 0.83 mmol) and LiOCH<sub>3</sub> (1.7 mmol, 1.7 mL of a 1 M solution in methanol) in methanol (15 mL) was added to a solution of CoCl<sub>2</sub>·6H<sub>2</sub>O (100 mg, 0.42 mmol) in methanol. The mixture was stirred at ambient temperature for 12 h, and the color changed to red-brown. Aerial oxidation of the reaction mixture resulted in a color change to blue. Addition of Et<sub>4</sub>NCl (70 mg, 0.42 mmol) in methanol (5 mL) yielded a blue precipitate. After filtration and drying in vacuo, complex **5a** was isolated as blue powder. Vapor diffusion of diethyl ether into a concentrated dmf solution of **5a** yielded crystals suitable for an X-ray diffraction study. Yield: 320 mg (76%). MS-MALDI (negative ions): *m/z* = 872 [M – Et<sub>4</sub>N<sup>+</sup>]<sup>−</sup>. UV/Vis (CH<sub>3</sub>OH): λ<sub>max</sub> (ε) = 324 (12.6), 369 (12.4), 654 nm.

**(Ph<sub>4</sub>As)[Co(**1b**)<sub>2</sub>] (5b):** A solution of H<sub>2</sub>-**1b** (312 mg, 1.0 mmol) and LiOCH<sub>3</sub> (2 mmol, 2 mL of a 1 M solution in methanol) in methanol (15 mL) was treated as described for **5a**. Addition of Ph<sub>4</sub>AsCl (209 mg, 0.5 mmol) in methanol (5 mL) yielded a blue solution. After removal of the solvent, the solid residue was washed extensively with diethyl ether and dried in vacuo to give **5b** a blue pow-

der. Yield: 260 mg (49%). MS-MALDI (negative ions):  $m/z$  = 680  $[M - \text{Ph}_4\text{As}^+]$ . UV/Vis ( $\text{CH}_3\text{OH}$ ):  $\lambda_{\text{max}}$  ( $\epsilon$ ) = 324 (13.2), 371 (13.6), 662 nm.

**(Et<sub>4</sub>N)<sub>2</sub>[Ni(1a)<sub>2</sub>] (6a):** A solution of H<sub>2</sub>-1 (409 mg, 1.0 mmol) and LiOCH<sub>3</sub> (2 mmol, 2 mL of a 1 M solution in methanol) in methanol (15 mL) was added to a solution of NiCl<sub>2</sub>·H<sub>2</sub>O (119 mg, 0.5 mmol). The mixture was stirred at ambient temperature for 12 h, and the color changed to red. Addition of Et<sub>4</sub>NCl (166 mg, 1.0 mmol) in methanol (5 mL) caused the formation of a red precipitate. After filtration and drying in vacuo, compound **6a** was isolated as a red solid. Yield: 340 mg (60%). <sup>1</sup>H NMR (200 MHz, [D<sub>7</sub>]dmf, 25 °C):  $\delta$  = 9.86 [t, 4 H, C(O)NH], 7.6–7.25 (m, 24 H, Ar-H), 4.64 (d, 8 H, NCH<sub>2</sub>Ph) 3.31 (q, 16 H, NCH<sub>2</sub>CH<sub>3</sub>), 1.24 (t, 24 H, CH<sub>2</sub>CH<sub>3</sub>) ppm. MS-MALDI (negative ions):  $m/z$  = 1002  $[M - \text{Et}_4\text{N}^+]$ . UV/Vis ( $\text{CH}_3\text{OH}$ ):  $\lambda_{\text{max}}$  ( $\epsilon$ ) = 315 (27.9), 385 (6.9), 870 nm.

**(Ph<sub>4</sub>As)<sub>2</sub>[Ni(1b)<sub>2</sub>] (6b):** A solution of H<sub>2</sub>-1b (312 mg, 1.0 mmol) and LiOCH<sub>3</sub> (2 mmol, 2 mL of a 1 M solution in methanol) in methanol (15 mL) was treated as described for **6a**. Addition of Ph<sub>4</sub>AsCl (418 mg, 0.5 mmol) in methanol (5 mL) gave a red solution. After removal of the solvent, the mixture was washed extensively with diethyl ether. Compound **6b** was obtained after drying in vacuo as a red powder. Yield: 250 mg (35%). <sup>1</sup>H NMR (200 MHz, CDCl<sub>3</sub>, 25 °C):  $\delta$  = 7.83 (m, 8 H, Ar-H), 7.75 (m, 24 H, Ar-H + NH), 7.56 (m, 16 H, Ar-H), 4.03 (sept, 2 H, CH), 1.16 (d, 24 H, CH<sub>3</sub>) ppm. MS-MALDI (negative ions):  $m/z$  = 1063  $[M - \text{Ph}_4\text{As}^+]$ . UV/Vis ( $\text{CH}_3\text{OH}$ ):  $\lambda_{\text{max}}$  ( $\epsilon$ ) = 310 (26.9), 370 (6.9), 864 nm. Vapor diffusion of diethyl ether into a concentrated dmf solution of **6b** yielded red crystals of **6b**·dmf, which were suitable for an X-ray diffraction study.

**(Ph<sub>4</sub>As)[Fe(1a)<sub>2</sub>] (7):** A solution of H<sub>2</sub>-1a (340 mg, 0.83 mmol) and LiOCH<sub>3</sub> (1.7 mmol, 1.7 mL of a 1 M solution in methanol) in methanol (15 mL) was added to a solution of FeCl<sub>3</sub> (68 mg, 0.42 mmol) in methanol. The mixture was stirred at ambient temperature for 12 h, and the color changed to red-brown. Addition of Ph<sub>4</sub>AsCl (176 mg, 0.42 mmol) in methanol (5 mL) yielded a red-brown precipitate. After filtration and drying in vacuo, complex **7** was isolated as a red-brown powder. Yield: 350 mg (66%). MS-MALDI (negative ions):  $m/z$  = 869  $[M - \text{Ph}_4\text{As}^+]$ . UV/Vis ( $\text{CH}_3\text{OH}$ ):  $\lambda_{\text{max}}$  ( $\epsilon$ ) = 320 (16.2), 391 (18.4), 491 nm. Vapor diffusion of diethyl ether into a concentrated dichloromethane solution of **7** yielded crystals of **7**·CH<sub>2</sub>Cl<sub>2</sub>, which were suitable for an X-ray diffraction study.

**Crystal Structure Determinations:** Single crystals suitable for X-ray diffraction analyses were coated in perfluoro polyether oil and mounted on glass fibers. Diffraction data were collected at  $T$  = 123(2) K (for **5a** and **7**·CH<sub>2</sub>Cl<sub>2</sub>) or at 153(2) K (for **6b**·dmf) with a Bruker AXS APEX CCD diffractometer equipped with a rotation anode using graphite-monochromated Mo- $K_\alpha$  radiation ( $\lambda$  = 0.71073 Å). Diffraction data were collected over the full sphere and were corrected for absorption. The data reduction was performed with the Bruker SMART<sup>[21]</sup> program package. Structures were solved with the SHELXS-97<sup>[22]</sup> package by using direct methods and were refined with SHELXL-97<sup>[22]</sup> against  $|F^2|$  by using first isotropic and later anisotropic thermal parameters for all non-hydrogen atoms. Hydrogen atoms were added to the structure models in calculated positions. CCDC-768615 (**5a**), -768616 (**6a**·dmf), and -768617 (**7**·CH<sub>2</sub>Cl<sub>2</sub>) contain the supplementary crystallographic data for this paper. These data can be obtained free of charge from The Cambridge Crystallographic Data Center via [www.ccdc.cam.ac.uk/data\\_request/cif](http://www.ccdc.cam.ac.uk/data_request/cif).

**Crystal Data for (Et<sub>4</sub>N)[Co(1a)<sub>2</sub>]:** C<sub>52</sub>H<sub>56</sub>CoN<sub>5</sub>O<sub>4</sub>S<sub>4</sub>,  $M$  = 1002.19 g mol<sup>-1</sup>, blue needles, space group  $P2_12_12_1$ ,  $a$  = 9.6136(13),

$b$  = 17.410(2),  $c$  = 28.357(4) Å,  $V$  = 4746.2(11) Å<sup>3</sup>,  $\rho$  = 1.403 g cm<sup>-3</sup>,  $\mu$  = 0.590 mm<sup>-1</sup>,  $Z$  = 4, 33702 measured reflections, 7023 unique reflections ( $R_{\text{int}}$  = 0.0684), 6593 observed reflections [ $I \geq 2\sigma(I)$ ], 628 parameters,  $R(\text{all})$  = 0.0538,  $wR(\text{all})$  = 0.0944, GOF = 1.167, largest peak/hole 0.386/−0.394 e<sup>-</sup> Å<sup>-3</sup>.

**Crystal Data for (Ph<sub>4</sub>As)<sub>2</sub>[Ni(1b)<sub>2</sub>]·dmf:** C<sub>79</sub>H<sub>83</sub>As<sub>2</sub>N<sub>5</sub>NiO<sub>5</sub>S<sub>4</sub>,  $M$  = 1519.29 g mol<sup>-1</sup>, red plates, space group  $P\bar{1}$ ,  $a$  = 13.351(3),  $b$  = 13.548(3),  $c$  = 23.883(6) Å,  $\alpha$  = 93.579(5),  $\beta$  = 103.481(5),  $\gamma$  = 114.970(5)°,  $V$  = 3744(2) Å<sup>3</sup>,  $\rho$  = 1.348 g cm<sup>-3</sup>,  $\mu$  = 1.301 mm<sup>-1</sup>,  $Z$  = 2, 30413 measured reflections, 13173 unique reflections ( $R_{\text{int}}$  = 0.0586), 9390 observed reflections [ $I \geq 2\sigma(I)$ ], 878 parameters,  $R(\text{all})$  = 0.0755,  $wR(\text{all})$  = 0.1078, GOF = 0.990, largest peak/hole 0.821/−0.368 e<sup>-</sup> Å<sup>-3</sup>.

**Crystal Data for (Ph<sub>4</sub>As)[Fe(1a)<sub>2</sub>]·CH<sub>2</sub>Cl<sub>2</sub>:** C<sub>69</sub>H<sub>58</sub>AsCl<sub>2</sub>FeN<sub>4</sub>O<sub>4</sub>S<sub>4</sub>,  $M$  = 1337.10 g mol<sup>-1</sup>, brown plates, space group  $P\bar{1}$ ,  $a$  = 14.161(3),  $b$  = 15.192(3),  $c$  = 16.041(4) Å,  $\alpha$  = 97.954(5),  $\beta$  = 100.902(5),  $\gamma$  = 110.294(4)°,  $V$  = 3099.5(12) Å<sup>3</sup>,  $\rho$  = 1.433 g cm<sup>-3</sup>,  $\mu$  = 1.047 mm<sup>-1</sup>,  $Z$  = 2, 25317 measured reflections, 10894 unique reflections ( $R_{\text{int}}$  = 0.0819), 6847 observed reflections [ $I \geq 2\sigma(I)$ ], 782 parameter,  $R(\text{all})$  = 0.1051,  $wR(\text{all})$  = 0.1225, GOF = 0.979, largest peak/hole 0.511/−0.553 e<sup>-</sup> Å<sup>-3</sup>.

## Acknowledgments

We thank the Deutsche Forschungsgemeinschaft (IRTG 1444) for financial support.

- [1] a) C. L. Beswick, J. M. Schulman, E. I. Stiefel, *Prog. Inorg. Chem.* **2004**, 52, 55–110; b) M. L. Kirk, R. L. McNaughton, M. E. Helton, *Prog. Inorg. Chem.* **2004**, 52, 111–212.
- [2] S. J. Nietner Burgmayer, *Prog. Inorg. Chem.* **2004**, 52, 491–537.
- [3] C. Faulmann, P. Cassoux, *Prog. Inorg. Chem.* **2004**, 52, 399–489.
- [4] a) K. Ray, T. Weyhermüller, F. Neese, K. Wieghardt, *Inorg. Chem.* **2005**, 44, 5345–5360; b) K. Ray, T. Weyhermüller, A. Goossens, M. W. J. Crajé, K. Wieghardt, *Inorg. Chem.* **2003**, 42, 4082–4087; c) B. S. Lim, D. V. Fomitchev, R. H. Holm, *Inorg. Chem.* **2001**, 40, 4257–4262.
- [5] a) F. E. Hahn, C. Schulze Isfort, T. Pape, *Angew. Chem. Int. Ed.* **2004**, 43, 4807–4810; b) F. E. Hahn, T. Kreickmann, T. Pape, *Dalton Trans.* **2006**, 769–771; c) T. Kreickmann, C. Diedrich, T. Pape, H. V. Huynh, S. Grimme, F. E. Hahn, *J. Am. Chem. Soc.* **2006**, 128, 11808–11819; d) C. Schulze Isfort, T. Kreickmann, T. Pape, R. Fröhlich, F. E. Hahn, *Chem. Eur. J.* **2007**, 13, 2344–2357; e) F. E. Hahn, B. Birkmann, T. Pape, *Dalton Trans.* **2008**, 2100–2102; f) F. E. Hahn, M. Offermann, C. Schulze Isfort, T. Pape, R. Fröhlich, *Angew. Chem. Int. Ed.* **2008**, 47, 6794–6797; g) B. Birkmann, A. W. Ehlers, R. Fröhlich, K. Lammertsma, F. E. Hahn, *Chem. Eur. J.* **2009**, 15, 4301–4311; h) B. Birkmann, W. W. Seidel, T. Pape, A. W. Ehlers, K. Lammertsma, F. E. Hahn, *Dalton Trans.* **2009**, 7350–7352; i) J. S. Gancheff, R. O. Albuquerque, A. Guerrero-Martínez, T. Pape, L. De Cola, F. E. Hahn, *Eur. J. Inorg. Chem.* **2009**, 43, 4043–4051; j) F. Hupka, F. E. Hahn, *Chem. Commun.*, in press; k) F. E. Hahn, T. Kreickmann, T. Pape, *Eur. J. Inorg. Chem.* **2006**, 535–539; l) B. Birkmann, R. Fröhlich, F. E. Hahn, *Chem. Eur. J.* **2009**, 15, 9325–9329; m) for a review on supramolecular structures with benzene-*o*-dithiolato ligands, see: T. Kreickmann, F. E. Hahn, *Chem. Commun.* **2007**, 1111–1120.
- [6] S. A. Baudron, N. Avarvari, P. Batail, *Inorg. Chem.* **2005**, 44, 3380–3382.
- [7] a) H. V. Huynh, W. W. Seidel, T. Lügger, R. Fröhlich, B. Wibel, F. E. Hahn, *Z. Naturforsch., Teil B* **2002**, 57, 1401–1408; b) W. W. Seidel, F. E. Hahn, T. Lügger, *Inorg. Chem.* **1998**, 37,

- 6587–6596; c) F. E. Hahn, W. W. Seidel, *Angew. Chem. Int. Ed. Engl.* **1995**, *34*, 2700–2703.
- [8] a) K. Mrkvová, J. Kameníček, Z. Šindelář, L. Kvitek, *Transition Met. Chem.* **2004**, *29*, 238–244; b) R. Eisenberg, Z. Dori, H. B. Gray, J. A. Ibers, *Inorg. Chem.* **1968**, *7*, 741–748.
- [9] a) H. Alves, D. Simão, I. C. Santos, V. Gama, R. T. Henriques, H. Novais, M. Almeida, *Eur. J. Inorg. Chem.* **2004**, 1318–1329; b) M. J. Baker-Hawkes, Z. Dori, R. Eisenberg, H. B. Gray, *J. Am. Chem. Soc.* **1968**, *90*, 4253–4259.
- [10] D. Sellmann, S. Fünfgelder, F. Knoch, M. Moll, *Z. Naturforsch., Teil B* **1991**, *46*, 1601–1608.
- [11] D. Sellmann, H. Binder, D. Häußinger, F. W. Heinemann, J. Sutter, *Inorg. Chim. Acta* **2000**, *300–302*, 829–836.
- [12] a) K. Ray, A. Begum, T. Weyhermüller, S. Piligkos, J. van Slagereen, F. Neese, K. Wieghardt, *J. Am. Chem. Soc.* **2005**, *127*, 4403–4415; b) D. Sellmann, T. Becker, F. Knoch, *Chem. Ber.* **1996**, *129*, 509–519; c) D. Sellmann, U. Kleine-Kleffmann, L. Zapf, G. Huttner, L. Zsolnai, *J. Organomet. Chem.* **1984**, *263*, 321–331.
- [13] a) D. T. Sawyer, G. S. Srivatsa, M. E. Bodini, W. P. Schaefer, R. M. Wing, *J. Am. Chem. Soc.* **1986**, *108*, 936–942; b) B. S. Kang, L. H. Weng, D. X. Wu, F. Wang, Z. Guo, L. R. Huang, Z. Y. Huang, H. Q. Liu, *Inorg. Chem.* **1988**, *27*, 1128–1130.
- [14] a) K. Ray, E. Bill, T. Weyhermüller, K. Wieghardt, *J. Am. Chem. Soc.* **2005**, *127*, 5641–5654; b) D. Sellmann, K. P. Peters, R. M. Molina, F. W. Heinemann, *Eur. J. Inorg. Chem.* **2003**, 903–907; c) H. Alves, D. Simão, H. Novais, I. C. Santos, C. Giménez-Saiz, V. Gama, J. C. Waerenborgh, R. T. Henriques, M. Almeida, *Polyhedron* **2003**, *22*, 2481–2486.
- [15] C.-M. Lee, C.-H. Hsieh, A. Dutta, G.-H. Lee, W.-F. Liaw, *J. Am. Chem. Soc.* **2003**, *125*, 11492–11493.
- [16] a) W. W. Seidel, F. E. Hahn, *J. Chem. Soc., Dalton Trans.* **1999**, 2237–2241; b) H. V. Huynh, C. Schulze-Isfort, W. W. Seidel, T. Lügger, R. Fröhlich, O. Kataeva, F. E. Hahn, *Chem. Eur. J.* **2002**, *8*, 1327–1335.
- [17] a) K. Wang, *Prog. Inorg. Chem.* **2004**, *52*, 267–314; b) M. J. Baker-Hawkes, E. Billig, H. B. Gray, *J. Am. Chem. Soc.* **1966**, *88*, 4870–4875.
- [18] N. G. Connelly, W. E. Geiger, *Chem. Rev.* **1996**, *96*, 877–910.
- [19] a) A. Dey, F. E. Jenney Jr., M. W. W. Adams, E. Babini, Y. Takahashi, K. Fukuyama, K. O. Hodgson, B. Hedman, E. I. Solomon, *Science* **2007**, *318*, 1464–1468; b) A. Dey, C. L. Roche, M. A. Walters, K. O. Hodgson, B. Hedman, E. I. Solomon, *Inorg. Chem.* **2005**, *44*, 8349–8354; c) M. A. Walters, C. L. Roche, A. L. Rheingold, S. W. Kassel, *Inorg. Chem.* **2005**, *44*, 3777–3779; d) T. Glaser, I. Bertini, J. J. G. Moura, B. Hedman, K. O. Hodgson, E. I. Solomon, *J. Am. Chem. Soc.* **2001**, *123*, 4859–4860.
- [20] D. M. Giolando, K. Kirschbaum, *Synthesis* **1992**, 451–452.
- [21] Bruker AXS, **2000**.
- [22] G. M. Sheldrick, *Acta Crystallogr., Sect. A* **2008**, *64*, 112–122.

Received: February 11, 2010  
Published Online: April 23, 2010